

1 COMPARATIVE PHYLOGEOGRAPHY OF THREE HOST SEA ANEMONES IN
2 THE INDO-PACIFIC

3 Running Title: Phylogeography of host sea anemones

4

5 MADELEINE A. EMMS^{1,2}, PABLO SAENZ-AGUDELO³, EMILY C. GILES³,
6 REMY GATINS^{1,4}, GERRIT B. NANNINGA^{2,8}, ANNA SCOTT⁵, JEAN-PAUL A.
7 HOBBS⁶, ASHLEY J. FRISCH⁷, SUZANNE C. MILLS^{8,9}, RICARDO BELDADE^{8,10}
8 & MICHAEL L. BERUMEN¹

9 ¹*Red Sea Research Center, King Abdullah University of Science and Technology,*
10 *Thuwal, 23955-6900, Saudi Arabia.* ²*Department of Zoology, University of*
11 *Cambridge, Cambridge, CB2 3EJ, United Kingdom.* ³*Instituto de Ciencias*
12 *Ambientales y Evolutivas, Universidad Austral de Chile, Valdivia, 5090000, Chile.*
13 ⁴*Department of Ecology and Evolutionary Biology, University of California Santa*
14 *Cruz 115 McAllister Way, Santa Cruz, CA 95060, USA.* ⁵*National Marine Science*
15 *Centre and Marine Ecology Research Centre, School of Environmental Science and*
16 *Engineering, Southern Cross University, PO Box 4321, Coffs Harbour, New South*
17 *Wales 2450, Australia.* ⁶*School of Molecular and Life Sciences, Curtin University,*
18 *Perth, Western Australia, Australia.* ⁷*Reef HQ, Great Barrier Reef Marine Park*
19 *Authority, Townsville, Queensland 4810, Australia.* ⁸*PSL Université Paris: EPHE-*
20 *UPVD-CNRS, USR 3278 CRIOBE.* ⁹*Laboratoire d'Excellence "CORAIL", France.*
21 ¹⁰*Estación Costera de Investigaciones Marinas and Center for Advanced Studies in*
22 *Ecology and Biodiversity, Las Cruces, Pontificia Universidad Católica de Chile,*
23 *Casilla 114-D, Santiago, CP 6513677, Chile.*

24

25 **Corresponding Author: Pablo Saenz-Agudelo: pablo.saenzagudelo@gmail.com**

26

27

28

29 ACKNOWLEDGMENTS

30 This research was supported by the KAUST Office of Competitive Research Funds
31 (OCRF) under Award No. CRG-1-2012-BER-002 and baseline research funds to
32 M.L.B. We thank Dr. Vanessa Robitzch Sierra (Universidad Austral de Chile) for her
33 generous help with the genetic analysis of the specimens. We also thank the staff at
34 the Bioscience CORE laboratory at King Abdullah University of Science and
35 Technology for their sequencing support. Lastly, we are grateful to Dream Divers and
36 many members of the Reef Ecology Lab at King Abdullah University of Science and
37 Technology, past and present, for their logistical support. All specimens from the Red
38 Sea and Djibouti were obtained in accordance with local regulations. For fieldwork in
39 the Maldives conducted during the first Maldives Reef Biodiversity Workshop, we
40 wish to thank the University of Milano-Bicocca Marine Research and High Education
41 Centre in Magoodhoo, the Ministry of Fisheries and Agriculture, Republic of

42 Maldives and the community of Maghoodhoo, Faafu Atoll. Samples from the
43 Maldives were collected under research permit OTHR30-D/INDIV/2014/185.
44 Sampling at Papua New Guinea was undertaken under a research visa issued by the
45 government of Papua New Guinea. Verbal permissions were granted by Mrs. Cecilie
46 Benjamin (Chair of the Board, Mahonia Na Dari Research and Conservation Centre,
47 Kilu) and Mr. Thomas Koi (Village Elder and representative of the Local Marine
48 Management). Samples collected from the Great Barrier Reef were permitted by the
49 Great Barrier Reef Marine Park Authority (permits G13/35980.1, P02/0025-4.0 and
50 LHIMP/R/2014/001). Samples from Christmas Island were collected under exemption
51 number 2087. Samples from Moorea (French Polynesia) were collected under permit
52 N 1111/MCE/ENV issued by the Ministère de la Culture et de l'Environnement.

53

54 DATA ACCESSIBILITY

55

56 The multilocus genotype tables for each species have been included as supporting
57 information as one single excel file.

58

59

60

61 **Aim**

62 The mutualistic relationship between anemones and anemonefishes is one of the most
63 iconic examples of symbiosis. However, while anemonefishes have been extensively
64 studied in terms of genetic connectivity, such information is lacking entirely for host
65 sea anemones. Here, we provide the first information on the broad-scale population
66 structure and phylogeographic patterns of three species of host sea anemone,
67 *Heteractis magnifica*, *Stichodactyla mertensii*, and *Entacmaea quadricolor*. We
68 evaluate if there is concordance in genetic structure across several distinct
69 biogeographic areas within the Indo-Pacific region and to what extent the observed
70 patterns may concur with those found for anemonefishes.

71 **Location**

72 Indo-Pacific, including the Red Sea.

73 **Taxon**

74 *Heteractis magnifica*, *Stichodactyla mertensii*, and *Entacmaea quadricolor*

75 **Methods**

76 Microsatellite markers and a combination of statistical methods including Bayesian
77 clustering, Isolation by Distance (IBD), Analysis of Molecular Variance (AMOVA),
78 and Principal Components Analysis (PCA) were used to determine population
79 structure. The congruence among distance matrices method (CADM) was used to
80 assess similarity in spatial genetic patterns among species.

81 **Results**

82 Significant population structure was identified in the three host anemone species.
83 Each species is likely composed of at least two genetic clusters corresponding to two
84 biogeographic regions, the Red Sea and the rest of the Indo-Pacific. Two of the three
85 anemone species seem to be experiencing admixture where the two main clusters
86 overlap (the Maldives). IBD analyses in the Red Sea revealed differences in gene flow
87 among species, suggesting more limited dispersal potential for *E. quadricolor* than for
88 *S. mertensii* and *H. magnifica*. Clonality is documented in *S. mertensii* for the first
89 time.

90 **Main conclusions**

91 This research documents the genetic population structure for three ecologically
92 important host sea anemones across the Indo-Pacific and provides valuable insights
93 regarding their biogeography and evolution. Specifically, we found high levels of
94 genetic divergence between populations across different biogeographic regions,
95 suggesting different evolutionary lineages within species. At the same time, common
96 geographic overlap of population structures suggests similar evolutionary histories
97 among all three species. Interestingly, the observed patterns are congruent to some
98 extent with structure reported for several anemonefish species, reflecting their close
99 ecological association.

100

101 **Keywords:** Actiniaria, biogeography, Cnidaria, connectivity, coral reef, gene flow,
102 Indo-Pacific, microsatellites, phylogeography, population genetics.

103

104

105

106

107

108 INTRODUCTION

109 The roles of historical, environmental, geological, and geographic barriers to
110 gene flow in shaping a species' genetic diversity and ultimately its distribution, can be
111 determined by comparing population structures between species with similar
112 distributions and ecological niches (Bermingham & Moritz, 2002; Arbogast &
113 Kenagy, 2008). For example, different species displaying similar patterns of spatial
114 population structure suggests the presence of congruent evolutionary phylogeographic
115 processes. Alternatively, differences in these patterns between species can provide
116 evidence for the relative importance of individual life history strategies or variance in
117 evolutionary histories among species that can be the result of different effects of
118 historical events (Dawson, Louie, Barlow, Jacobs, & Swift, 2002; Crandall, Frey,
119 Grosberg, & Barber, 2008; Hui et al., 2016).

120 The Indo-Pacific is a highly diverse biogeographical region that includes the
121 Coral Triangle biodiversity hotspot, the Red Sea, and tropical waters of the Indian
122 Ocean, as well as the central and western Pacific (Hui et al., 2016). It is a broad
123 region with a complex geological history (Hall, 2002), and it encompasses different
124 bodies of water that together represent a mosaic of environmental conditions,
125 geographic settings, and oceanographic features (Bowen et al., 2016). Genetic surveys
126 show that the population structure of Indo-Pacific species can coincide with known
127 historical geological processes, geographical barriers or environmental gradients. For
128 example, low sea levels during glaciations exposed the Sunda (southeast Asia) and
129 Sahul (Australia-New Guinea) continental shelves (Voris, 2000) creating what is
130 known as the Indo-Pacific barrier or the Sunda Shelf barrier (Randall, 1998; Rocha,
131 Craig, & Bowen, 2007). Several studies in different marine fishes and invertebrates
132 have shown a geographic concordance of population genetic structure with this
133 historical barrier with populations in the Pacific being divergent from those in the
134 Indian Ocean (reviewed in Ludt & Rocha, 2015; Crandall et al., 2019). More
135 precisely, documented genetic breaks occur in the eastern Indian Ocean (Christmas
136 Island, Cocos Keeling Islands, Indonesia), representing the division between Indian
137 Ocean and Pacific populations. This division has been attributed to changes in sea-
138 level during the Plio-Pleistocene which resulted in land bridges throughout Indonesia
139 that effectively split Indo-Pacific groups into allopatric Indian and Pacific populations
140 or species (Rocha et al., 2007; Gaither & Rocha, 2013). Similarly, the narrow,
141 shallow Bab-el-Mandab strait (between the Red Sea and western Indian Ocean), has
142 been considered an historical barrier to gene flow to numerous species that display
143 genetic structure between populations in the Red Sea and in the Indian Ocean
144 (Klausewitz, 1989; DiBattista et al., 2016). Yet, despite being widespread across the
145 Indo-Pacific, there is no available information about the distribution of genetic
146 diversity of sea anemones or the role played by historical/geological barriers.

147 Geographic and environmental settings have also been documented as barriers
148 to gene flow. For instance, the large geographic distances separating some Pacific
149 islands, such as Moorea (French Polynesia), the Marquesas Islands, and Easter Island,
150 represent geographic barriers to gene flow (Randall 1998; Rocha et al., 2007).

151 Barriers to gene flow have also been identified in the Red Sea, and these are linked to
152 environmental gradients (Saenz-Agudelo et al. 2015). Several studies have shown
153 correlations between genetic distance and these environmental gradients (Nanninga,
154 Saenz-Agudelo, Manica, & Berumen, 2014; Giles, Saenz-Agudelo, Hussey, Ravasi, &
155 Berumen, 2015; Sawall, Al-Sofyani, Banguera-Hinestroza, & Voolstra, 2014; Reimer
156 et al., 2017). However, again, the role of geographic barriers in shaping the genetic
157 diversity of sea anemones has not been examined.

158 Many marine species are endemic to the Indo-Pacific region and some of these
159 have evolved symbiotic relationships, such as the iconic association between host sea
160 anemones (Order Actiniaria) and anemonefishes (Genera *Amphiprion* and *Premnas*;
161 Fautin & Allen, 1997; Allen, Drew, & Fenner, 2010). A number of studies report
162 large-scale population genetic structure of anemonefishes (Timm & Kochzius, 2008;
163 Nanninga et al., 2014; Dohna, Timm, Hamid, & Kochzius, 2015; Saenz-Agudelo et
164 al., 2015; Steinberg et al., 2016; Huyghe & Kochzius, 2017; O'Donnell, Beldade,
165 Mills, Williams, & Bernardi, 2017). In general these studies indicate that anemonefish
166 species such as *Amphiprion bicinctus*, *Amphiprion ocellaris*, and *Amphiprion*
167 *perideraion* display genetic structure that coincides with historical geographic barriers
168 such as the Sunda shelf, the Strait of Bab Al Mandeb, between basins (Pacific
169 Ocean and Indian Ocean) or between the eastern and western sides of the Indian
170 Ocean. In contrast, there is a limited understanding of the dispersal abilities and
171 population connectivity of their host sea anemones, and whether or not there are
172 similarities in their genetic structure with that of anemonefishes. Resolving these
173 knowledge gaps could shed light on the processes that have shaped their close
174 ecological relationship.

175 Population structure, re-colonization, and replenishment of host sea anemones
176 are influenced by dispersal and reproduction. Of the few reproduction studies that
177 have been conducted, *Entacmaea quadricolor* and *Heteractis crispa* were found to be
178 gonochoric, releasing their gametes in broadcast spawning events in the austral
179 summer and autumn in subtropical Australia (Scott & Harrison, 2005, 2007, 2009). In
180 the Red Sea, male *Stichodactyla mertensii* have been observed spawning on three
181 consecutive days after a boreal spring full moon (Bouwmeester, Gatins, Giles,
182 Sinclair-Taylor, & Berumen, 2016). In the laboratory, most *E. quadricolor* planulae
183 metamorphose within two weeks, although they can remain free-swimming for at
184 least two months (Scott & Harrison, 2007). This suggests that anemone larvae have
185 the potential to travel large distances, potentially facilitating high levels of gene flow,
186 though larval dispersal may be more restricted when asexual reproduction is common.
187 *Heteractis magnifica* and *E. quadricolor* can reproduce asexually using longitudinal
188 fission (Scott, 2017) and the resulting clones can form large assemblages of >100
189 individuals (Frisch et al., 2019).

190 In this study, we determine the broad-scale genetic structure and
191 phylogeography of three host anemone species (*H. magnifica*, *S. mertensii*, and *E.*
192 *quadricolor*) and test for congruence in genetic structure among species and genetic
193 divergence associated to putative barriers previously reported for other coral reef
194 organisms. Our hypothesis is that given the large geographic distribution of these
195 species, these anemones should display some degree of genetic structure across their
196 distribution range and this structure should be concordant with the well-characterized
197 biogeographic breaks and also with the genetic structure of the anemonefishes that
198 these species host.

199

200 MATERIALS AND METHODS

201 *Heteractis magnifica*, *S. mertensii*, and *E. quadricolor* are widely distributed
202 across the Indo-Pacific and Red Sea. *H. magnifica* occupies the largest longitudinal
203 range of the three species, from French Polynesia to East Africa and the Red Sea,
204 while *S. mertensii* and *E. quadricolor* range from Micronesia and Melanesia to East
205 Africa and the Red Sea (Fautin & Allen, 1992; Brolund, Tychsen, Nielsen, &
206 Arvedlund, 2004; Gatins, Saenz-Agudelo, Scott, & Berumen, 2018). All three species
207 are present from Australia to the Ryukyu Islands, with *E. quadricolor*'s distribution
208 extending further north to Japan (Fautin & Allen, 1992). All three species can be
209 found in extremely shallow waters around 1 m deep (Dunn, 1981) but maximum
210 depths vary. *Heteractis magnifica* and *E. quadricolor* can inhabit mesophotic waters
211 down to around 60 m (Brolund et al., 2004; Bridge, Scott, & Steinberg, 2012), while
212 *S. mertensii* are limited to shallow waters of around 20 m (Dunn, 1981). Tentacle
213 specimens were collected using dissecting scissors and forceps whilst SCUBA diving
214 at 42 sites across the Indo-Pacific and Red Sea (Fig. 1 & Table 1). Specimens were
215 placed in 2 ml vials and stored in 96% ethanol. The GPS coordinates of each anemone
216 were also recorded.

217 DNA was extracted from 880 specimens using Qiagen's DNeasy Blood and
218 Tissue Kit according to the manufacturer's protocol. A total of 10 unique
219 microsatellite markers were amplified for *H. magnifica*, 11 for *S. mertensii*, and 12 for
220 *E. quadricolor* (Table S1, Supporting information). All forward sequences were
221 labelled with a fluorescent dye (6-FAM, NED, PET, VIC). PCR conditions followed
222 the Qiagen PCR Multiplex kit protocol with modifications as in Gatins et al. (2018); a
223 total of 10 μ L was used for each individual reaction mix, including 5 μ L of Multiplex
224 PCR MasterMix (Qiagen), 1 μ L of primers (2 μ M; see Table S1, Supporting
225 information), 3.3 μ L of water and 0.7 μ L DNA (50-150 ng/ μ L). The thermocycler
226 conditions for PCR amplifications were: 95 $^{\circ}$ C for 15 min, then 25 cycles of 94 $^{\circ}$ C for
227 30 s, annealing at a locus-specific temperature (57/60 $^{\circ}$ C, see Table S1, Supporting
228 information) for 90 s, and an extension at 72 $^{\circ}$ C for 60 s, with a final extension set at
229 60 $^{\circ}$ C for 30 min. Further details regarding microsatellite and PCR protocols can be
230 found in Gatins et al. (2018). Final PCR products of 10 μ L were diluted with 130 μ L
231 MilliQ water before being sent for fragment size analysis using a GeneScan 500-LIZ
232 size standard and an ABI 3730xl genetic analyser (Applied Biosystems, USA) in the
233 Biosciences CORE laboratory at King Abdullah University of Science and
234 Technology, Saudi Arabia. Genotyping was completed using Geneious v. 8.1.6
235 (Kearse et al., 2012).

236 The final datasets consisted of 205 *H. magnifica* individuals, 122 *S. mertensii*
237 individuals, and 249 *E. quadricolor* individuals (Table 1; samples with more than
238 three missing loci were excluded). Clonality was investigated and corrected for by
239 comparing multilocus genotypes in GenAlEx v.6.502 (Peakall & Smouse, 2012).
240 Subsequent analyses were conducted using the corrected datasets, leaving only one
241 individual per multi-locus genotype. GenePop v.4.2 (Raymond & Rousset, 1995;
242 Rousset, 2008) was used to check for deviations from Hardy-Weinberg Equilibrium
243 (HWE), and thus the presence of null alleles. Calculations of the inbreeding
244 coefficient F_{IS} (Weir & Cockerham, 1984), deviations from HWE, and linkage
245 disequilibrium in pairwise comparisons of all loci were also tested for using GenePop.
246 Significance values were estimated using Markov chain methods (1000
247 dememorizations, 100 batches, and 1000 iterations per batch) and were adjusted in R
248 using the false discovery rate (fdr) method (Benjamini & Hochberg, 1995; alpha =

249 0.05). Summary statistics, including allelic richness, expected and observed
250 heterozygosity, and fixation indices were calculated in GenAlEx. At some locations it
251 was not possible to obtain the minimum requirement of five specimens. We did not
252 estimate summary statistics for these sites to avoid biases associated with small
253 sample sizes.

254 For each species' dataset, the software Structure v. 2.3.4 (Pritchard, Stephens,
255 & Donnelly, 2000) was used to perform a Bayesian clustering analysis to estimate the
256 most likely number of genetic clusters or putative populations (K) given the genotypic
257 data. Parameters were set to use the admixture model with sampling location as prior
258 and correlated allele frequencies. Analyses were run with a burn-in period of 200,000
259 iterations, 500,000 MCMC repetitions, K set to the number of sites sampled, and five
260 runs for each value of K for each species. The resulting data were uploaded to
261 Structure Harvester (Earl, 2012) in order to summarize and visualize the change in the
262 mean log likelihood and Evanno's delta K for different population clusters (K).
263 CLUMPAK (Kopelman, Mayzel, Jakobsson, Rosenberg, & Mayrose, 2015) was then
264 used to create a visual representation of the population structure based on several
265 estimates of K, combining the data files (runs) from Structure. We used Principal
266 Component Analysis (PCA) to depict the overall genetic variability among
267 individuals, as an alternative to Structure that has no underlying assumptions to
268 identify genetic structures (Jombart, Devillard, & Balloux, 2010). To do this, we used
269 the `dudi.pca` function of the `ade4` package available in R (Chessel, Dufour, &
270 Thioulouse, 2004). An Analysis of Molecular Variance (AMOVA) was performed in
271 GenAlEx (Peakall & Smouse, 2012) to quantify the magnitude of genetic variation
272 among the groups identified by structure and among locations. Our intention with this
273 analysis was to provide an indication of the magnitude of genetic divergence between
274 clusters identified by structure and compares it among species (Meirmans, 2015). The
275 same program was used to estimate pairwise F_{ST} (Wright, 1965), and F'_{ST} (Meirmans,
276 2006).

277 The congruence among distance matrices (CADM, Legendre & Lapointe,
278 2004) method was used to quantify the similarity in genetic structure patterns among
279 the three species. This was conducted using the R package 'ape' 3.0 (Paradis, Claude,
280 & Strimmer, 2004). Here, a coefficient of concordance among all matrices (Kendall's
281 W) is generated and ranges from zero to one. Zero indicates no concordance and one
282 indicates complete concordance (Kendall & Smith, 1939). A posteriori tests of
283 pairwise similarity among matrices (r_M) were then conducted. For tests of congruence,
284 distance matrices (F_{ST}) were generated for only the co-sampled sites where at least
285 three samples were collected for each of the three species ($n= 4$ sites). The Holm
286 (1979) method was used to correct P-values following multiple testing.

287 Correlations between pairwise genetic differentiation and geographic distances
288 were estimated for each species (Isolation by Distance, IBD) in the Red Sea. We did
289 this to evaluate whether patterns of genetic structure differed among species at a
290 smaller scale. We ran this analysis in the Red Sea because this is the only region
291 where sample coverage was sufficient to compare IBD patterns among species. For
292 this analysis, we estimated pairwise genetic and geographic distance matrices for each
293 species for all sites that had at least five specimens (after clone correction). We used
294 F'_{ST} (Meirmans, 2006) for genetic distances, a standardized estimate of genetic
295 differentiation that accounts for genetic variation within populations and enables
296 comparisons among different datasets. We used shortest overwater distances in
297 kilometres for geographic distances. We explored IBD for each species using Mantel

298 tests with 10,000 permutations to test for significant correlations between distance
299 matrices.

300

301 RESULTS

302 *Clonality and allelic richness*

303 We found evidence of clonality across all species despite no prior record of
304 clonality in *S. mertensii*. *Heteractis magnifica* had the highest proportion of clones,
305 with the highest rates in Moorea (French Polynesia) (13 out of 26; 50%) and at Red
306 Sea sites (58 out of 120; 48%); clones were also present at Djibouti (2 out of 5; 40%).
307 Two *S. mertensii* clone pairs were identified. One in Fi'ran (Red Sea) and a second
308 pair in Djibouti. *Entacmaea quadricolor* clones were mostly found in the Indian
309 Ocean (3 out of 7; 43%) and eastern/southeastern Australia (13 out of 77; 17%), as
310 well as and one in Fsar (Red Sea) (Table 1). In general, *H. magnifica* clones were
311 more common at the periphery of its distribution while *E. quadricolor* clones were
312 found in the Indian Ocean and across the eastern Indo-Pacific.

313 Overall, after clone removal, there were no consistent deviations from HWE
314 for any given locus in any of the three species. We found no consistent evidence for
315 linkage between pairs of loci across multiple sites for any of the three species and thus
316 all loci were kept for further analyses. Summary statistics across loci per sampling site
317 are provided in Table S2 (Supporting information). Briefly, highest mean allelic
318 richness across loci for *H. magnifica*, *S. mertensii*, and *E. quadricolor* was found at
319 Kimbe Island, Lizard Island, and Jazirat Burcan, respectively, while the lowest was
320 found in Obhur and Dumsuq for *H. magnifica*, Abu Dauqa, Abu Madafi, and Dhi
321 Dahaya for *S. mertensii*, and Abrolhos Island for *E. quadricolor*. Highest observed
322 heterozygocities were in Moorea, Kimbe Island, and North Solitary Island,
323 respectively, while lowest observed heterozygosities were in Fsar, Djibouti, and
324 Kimbe Island.

325

326 *Broad-scale genetic structure*

327 *Heteractis magnifica*, *S. mertensii*, and *E. quadricolor* all formed at least two
328 main genetic groups across the Indo-Pacific, and these groups were arranged
329 geographically (Fig. 2). When K was set to 2, for all species, the Red Sea sites and
330 Djibouti (when sampled) clustered together in one group (hereafter referred to as the
331 Red Sea cluster). For all species the main genetic break coincided at the Maldives.
332 Interestingly, *H. magnifica* and *S. mertensii* showed evidence of admixture at the
333 Maldives between the two genetic groups while *E. quadricolor* did not (one sample
334 clustered with specimens from the Indo-Pacific while the other specimens clustered
335 together with the Red Sea). Further genetic structure was revealed when K was
336 increased (Fig. 2). For *H. magnifica*, specimens from Moorea (French Polynesia)
337 clustered as a separate group when K was set to 3 and 4, and the Maldives clustered as
338 a separate (admixed) group when K was set to 4 (Fig. 2A). For *S. mertensii*, setting K
339 to 3 suggested weak structure within the Red Sea (Gulf of Aqaba appeared different
340 from other locations) and setting K to 4 resulted in clustered specimens from the
341 Maldives and the Bismarck Sea with varying degrees of admixture (Fig. 2B). For *E.*
342 *quadricolor*, setting K to 3 clustered together the specimens from Abrolhos Island
343 (eastern Indian Ocean), the Bismarck Sea, and Lizard Island (north Great Barrier

344 Reef) in one group and specimens from Lord Howe Island (southeastern Australia) in
345 another group. Specimens from the Keppel, Northwest, and Heron Islands (southern
346 Great Barrier Reef) and North Solitary Island (eastern Australia) appear to have
347 admixed genotypes from Lizard and Lord Howe Islands (with a major proportion
348 being from the Lord Howe cluster). Interestingly, a few individuals from Keppel and
349 North Solitary Islands also showed potential admixture with the Red Sea cluster.
350 Setting K to 4 showed a clear isolation by distance pattern within Red Sea sites (Fig.
351 2C). Mean log likelihood and Evanno's Delta K plots for K = 1 to K = 25 from
352 Structure runs can be found in Supporting information (Fig. S1). Structure barplots for
353 K = 5 to K = 8 for all species can be found in Supporting Information (Fig. S2, Fig.
354 S3 and Fig. S4). According to Evanno's Delta K the most likely number of clusters
355 for all three species is 2.

356 PCA provided similar results to Structure. For all species, Red Sea specimens
357 clustered together with Djibouti and separately from the rest of the specimens. Denser
358 clusters indicate less genetic variation among individuals compared to other locations.
359 For *H. magnifica*, specimens from Moorea (French Polynesia) formed a distinct
360 cluster from all other Pacific specimens, and specimens from the Maldives fell
361 between the Bismarck Sea specimens and the Red Sea specimens (Fig. 3A). For *S.*
362 *mertensii*, there is greater genetic variation between individuals outside the Red Sea
363 with separation between specimens from the Bismarck Sea and the Pacific but with
364 some degree of overlap. Specimens from the Indian Ocean fell in between the Red
365 Sea cluster and the rest of the specimens but closer to the Pacific specimens (Fig. 3B).
366 Finally, for *E. quadricolor*, there was separation between specimens from the Pacific
367 and Indian Oceans, and the specimens from the Bismarck Sea fell in between these
368 two groups with some specimens overlapping with each of these two groups (Fig.
369 3C). All *E. quadricolor* regions within the Indo-Pacific appeared to cluster almost
370 equidistant to the Red Sea, with a few specimens from the Indian Ocean and the
371 Pacific clustered within it, as expected from the Structure results.

372

373 *Partitioning of genetic variation*

374 Results from hierarchical AMOVAs that included two regions (the Red Sea
375 and the rest of the Indo-Pacific) indicated that genetic variation (other than that within
376 individuals; >43%) among regions differed considerably among species. The lowest
377 variation among groups was for *H. magnifica* (14%; $F_{RT} = 0.143$), followed by *E.*
378 *quadricolor* (22%; $F_{RT} = 0.220$) and finally *S. mertensii* (42%; $F_{RT} = 0.408$).
379 Interestingly, the amount of genetic variation explained by differences among
380 populations within groups did not display the same patterns as variation among
381 regions. *Stichodactyla mertensii* displayed the lowest variation at this level (1.1%, F_{RS}
382 = 0.019), followed by *E. quadricolor* (5%; $F_{SR} = 0.064$) and then *H. magnifica* (9.7%;
383 $F_{RS} = 0.113$). Global F_{ST} values were lower for *H. magnifica* ($F_{ST} = 0.240$) and *E.*
384 *quadricolor* ($F_{ST} = 0.270$) compared to *S. mertensii* ($F_{ST} = 0.419$) (Table 2).

385 In all three species, all pairwise F_{ST} comparisons that involved one site from
386 the Red Sea and one from elsewhere were statistically greater than zero after fdr
387 corrections (Table S3, Supporting information). Highest pairwise F_{ST} and F'_{ST} values
388 were found between Obhur (Red Sea) and Moorea (French Polynesia) for *H.*
389 *magnifica* ($F_{ST} = 0.384$ and $F'_{ST} = 0.749$, respectively), between Obhur and Lizard
390 Island (northern Great Barrier Reef) and Abu Madafi (Red Sea) and Lizard Island for
391 *S. mertensii* ($F_{ST} = 0.427$ and $F'_{ST} = 0.823$), and between Dhi Dahaya (Red Sea) and

392 Lord Howe Island (southeastern Australia) for *E. quadricolor* ($F_{ST} = 0.347$ and $F'_{ST} =$
393 0.736). Lowest F_{ST} and F'_{ST} values were consistently found between sites within the
394 Red Sea for all three species (Table S3, Supporting information).

395

396 *Congruence among genetic distances and Isolation By Distance in the Red Sea*

397 Concordance based on genetic distance (F_{ST}) was high and significant among
398 the three species ($W = 0.82$, $X^2 = 12.33$, adjusted $p = 0.011$). Pairwise similarity among
399 matrices tested a posteriori was also high, ranging from 0.657-0.771, but was only
400 significant for the comparison of *E. quadricolor* and *S. mertensii*. Given this, we can
401 only reject the null hypothesis of no concordance for *E. quadricolor* and *S. mertensii*
402 that, from this test, appear to display very similar patterns of genetic structure based
403 on F_{ST} . Comparing pairwise F'_{ST} values among species and as a function of
404 geographic distance in the Red Sea revealed differences among species (Fig. 4). Only
405 *E. quadricolor* displayed a positive correlation between genetic and geographic
406 distance within the Red Sea cluster (Fig. 4 & Table S4, Supporting information).

407

408 DISCUSSION

409 This study represents the first broad-scale study of the population genetics of
410 sea anemones that provide essential habitat for anemonefishes. Significant population
411 structure was identified in *H. magnifica*, *S. mertensii*, and *E. quadricolor* across the
412 Indo-Pacific. Our data indicate the existence of at least two geographically segregated
413 genetic groups for all species, namely the Red Sea cluster and the rest of the Indo-
414 Pacific cluster. Interestingly, the major genetic break that separates these two clusters
415 coincides at the Maldives. Overall, our results indicate widespread connectivity of *H.*
416 *magnifica*, *S. mertensii*, and *E. quadricolor* within the Red Sea cluster and to a lesser
417 extent within the rest of the Indo-Pacific. Below we compare and discuss the
418 differences in genetic structure among the three anemone species studied and discuss
419 how our findings complement our current understanding of the phylogeography and
420 population connectivity in the Indo-Pacific and Red Sea regions.

421 The abundance and location of clones varied among the three host anemone
422 species. *Heteractis magnifica* clones were restricted to the periphery of their ranges,
423 which agrees with Dunn (1981). These sites likely experience limited gene flow,
424 which may decrease the chances of successful larval recruitment and increase the
425 importance of asexual reproduction (Hoffmann, 1986; Eckert, 2001; Billingham,
426 Reusch, Alberto, & Serrão, 2003; Johannesson & André, 2006). In contrast, *E.*
427 *quadricolor* clones were found across their range including at central sites in the
428 Indian Ocean, which may be explained by Dunn's (1981) additional observation that
429 *E. quadricolor* clonality varies with depth rather than geographical location. As
430 reflected by our findings, a sea anemone's ability to undergo asexual reproduction is
431 species-specific and dependant on the ecological conditions found at each habitat
432 throughout a particular species' range (Sebens, 1980). In general, clusters of *H.*
433 *magnifica* and *E. quadricolor* appear to be common (Harriott, & Harrison, 1997;
434 Brolund et al., 2004; Richardson, Scott & Baird, 2015), and this seems to be
435 consistent with our results in terms of proportions of clones found. Neither asexual
436 reproduction nor clusters of several individuals have been documented before in *S.*
437 *mertensii*. Together with the low levels of clonality in *S. mertensii* reported in this
438 study it seems that this mode of reproduction is rare in this species.

439 We found that there is a significant congruence of patterns of genetic
440 differentiation among species and that the Maldives (western/central Indian Ocean)
441 represents a location of overlap or possible hybridization among distinct anemone
442 populations or lineages (Sheppard et al., 2013). Previous studies have reported genetic
443 discontinuity between the eastern and western Indian Ocean in different taxa
444 including coral reef fishes (Bay, Choat, van Herwerden, & Robertson, 2004; Leray et
445 al., 2010; Gaither et al., 2011; Huyghe & Kochzius, 2017) and invertebrates such as
446 echinoderms (Vogler et al., 2012; Otwoma & Kochzius, 2016) and giant clams (Hui et
447 al., 2016). Only one of these included samples from the Maldives (Vogler et al., 2012)
448 and did not report overlap of different clades at these islands. Since none of the other
449 studies sampled the Maldives it is not possible to confirm whether genetic
450 discontinuity and the co-occurrence of different lineages at the Maldives is expected
451 for other taxa. Other studies describe the presence of genetic discontinuities towards
452 the eastern Indian Ocean (Christmas Island, Cocos Keeling Islands, Indonesia) for
453 other coral reef species such as fishes, echinoderms, molluscs, and arthropods
454 (reviewed in Ludt & Rocha, 2015; Crandall et al., 2019). However, most of the
455 studies that document this break did not include specimens from the western Indian
456 Ocean. Taken together, differences among studies are most likely due to the lack of
457 consistency in sampling efforts among taxa and studies in this region, as pointed out
458 by Crandall et al. (2019). This is a main limitation to draw general conclusions when
459 comparing patterns of genetic structure that can only be resolved through better
460 coordination among research groups. Our results are in agreement with previous
461 studies and suggest that genetic exchange among eastern and western Indian Ocean
462 might be limited by the presence of only a few islands that could facilitate
463 connectivity via island hopping (Sheppard et al., 2013; Otwoma & Kochzius, 2016).
464 The Maldives seems to be one of these important crossroads where different lineages
465 meet. Yet, this hypothesis remains to be tested further as limited or ancient dispersal
466 events are not the only possible processes that could have produced the observed
467 genetic structure and our sampling size at several locations is small.

468 We can only speculate as to why there was no genetic admixture in *E.*
469 *quadricolor* at the Maldives. Our data are limited (only four specimens), but suggest
470 that both lineages coexist in the same place. It is possible that for *E. quadricolor*,
471 these two clusters are the result of lineages that may have achieved reproductive
472 isolation while ongoing gene flow is still possible for *H. magnifica* and *S. mertensii*.
473 In this sense, IBD results indicate that *E. quadricolor* has more limited dispersal than
474 *H. magnifica* and *S. mertensii* within the Red Sea. However, given our uneven
475 sampling design among species, these results should be interpreted with caution.
476 These differences could be explained either by variation in pelagic larval duration
477 among species or variation in relative species abundance. *Entacmaea quadricolor*
478 larvae can settle 48 hours after spawning; yet, they can remain in the plankton for up
479 to 57 days (Scott & Harrison, 2007). However, little is known about larval dispersal
480 of the other two species and no information is available regarding relative abundances
481 of these anemones in the regions we sampled. Assuming that population connectivity
482 is mostly driven by larval exchange, and that differences in abundance of these three
483 species are negligible it appears that *H. magnifica* and *S. mertensii* larvae may have
484 higher dispersal potential than *E. quadricolor* larvae. This higher restriction in gene
485 flow might have facilitated the appearance of reproductive isolation among *E.*
486 *quadricolor* clades. However, these hypotheses require further investigation.

487 The genetic structure and evolutionary history of host anemones and
488 anemonefishes should be inextricably linked due to the obligate nature of the

489 symbiosis for the anemonefishes. We found at least three cases where there are
490 similarities in the genetic structure of anemonefishes and that of their host anemones
491 that warrant discussion. First, a previous study also employing microsatellite markers
492 has reported isolation by distance and environment within the Red Sea for
493 *Amphiprion bicinctus* (Nanninga et al., 2014), which inhabits *H. magnifica*, *E.*
494 *quadricolor*, *S. mertensii*, and to a lesser extent *Heteractis crispa* and *Heteractis*
495 *aurora*. IBD has been reported for other anemonefishes (Pinsky, Montes, Jr., &
496 Palumbi, 2010; Pinsky et al., 2017) and has been attributed to the relatively short
497 pelagic larval duration of these species (aprox. 12d). Here, only *E. quadricolor*
498 displayed IBD in the Red Sea suggesting a shorter PLD compared to the other
499 anemones and perhaps similar to the PLD of *A. bicinctus*. Second, deep genetic
500 differences between the eastern and western Indian Ocean have been reported for
501 *Amphiprion akallopisos* (Huyghe & Kochzius, 2017), which inhabits both *S. mertensii*
502 and *H. magnifica*. This coincides with our results, however the lack of samples of *A.*
503 *akallopisos* from the Maldives leaves the question open as to whether these two
504 lineages of *A. akallopisos* meet at the Maldives as seems to be the case for the three
505 anemone species in this study. Third, it has been shown that populations of the only
506 anemonefish species present in Moorea (French Polynesia), *Amphiprion chrysopterus*,
507 appear to be clearly different from populations elsewhere (Litsios, Pearman,
508 Lanterbecq, Tolou, & Salamin, 2014). This coincides with our finding that the
509 population of *H. magnifica* from Moorea is highly divergent from other *H. magnifica*
510 populations. Similarly, moderate genetic structure in *E. quadricolor* was found
511 between Lord Howe Island (located in southeastern Australia and to which
512 *Amphiprion mccullochi* is endemic), and locations along the Great Barrier Reef
513 (where its closest relative *Amphiprion akindynos* is commonly found) (van der Meer,
514 Jones, Hobbs, & van Herwerden, 2012). As pointed out previously, there is limited
515 geographic overlap between our study and previous studies of broad scale genetic
516 structure in anemonefishes that prevent us from making thorough comparisons, but
517 our results do suggest that there are some similarities in terms of genetic structure
518 among anemonefishes and their host sea anemones.

519 Studies of population genetics in the Indo-Pacific region have demonstrated
520 variation in patterns of genetic differentiation across a broad range of species, with
521 evidence of several genetic breaks including between the Indian and Pacific Oceans,
522 between the Red Sea and the Indian Ocean, and between sub-regions of the Indian
523 Ocean (reviewed in Crandall et al., 2019). Here, we studied the broad-scale
524 population genetics of host anemone species for the first time and identified distinct
525 genetic groups with deep divergences at least between the Red Sea and the rest of the
526 Indo-Pacific region and possibly also in Moorea. These deep divergences suggest
527 possible species complexes within these species, which has also been suggested at
528 least for *E. quadricolor* in a recent phylogenetic reconstruction of the clownfish
529 hosting sea anemones (Titus et al., 2019). Overall, the patterns of population structure
530 documented here are similar across *H. magnifica*, *S. mertensii*, and *E. quadricolor*,
531 suggesting shared evolutionary processes. These divergences coincide with the
532 Western Indian / Western Indo-Pacific barrier and the Central Indo-Pacific / Eastern
533 Indo-Pacific biogeographic barriers and are most likely the result of complex changes
534 involving larval connectivity and population sizes associated with Pleistocene sea-
535 level fluctuations (Ludt & Rocha, 2015). The incongruence of our findings compared
536 to other coral reef associated taxa that display genetic discontinuities elsewhere (such
537 as the Sunda shelf) is most likely associated to differences among species linked to
538 genetic drift (Crandall et al., 2019). Within the identified groups, connectivity is

539 relatively high for all species, but seems to be more restricted in *E. quadricolor* than
540 in the other two species, at least in the Red Sea. However, our results need to be
541 interpreted with caution because our sampling scheme was limited in terms of the
542 number of samples per location and the congruence of sampling sites among different
543 anemone species. Clearly further studies are needed to elucidate the role of
544 evolutionary forces and demographic history in shaping the genetic structure of
545 populations of these three sea anemones. We hope that our results serve as a road map
546 to further develop these questions regarding the drivers of evolution and population
547 structure of host sea anemones.

548

549 TABLES

550 Table 1. Summary of specimens for *Heteractis magnifica*, *Stichodactyla mertensii*,
 551 and *Entacmaea quadricolor* across the Indo-Pacific, including number of specimens
 552 successfully genotyped (N) and number of unique genotypes following clone
 553 correction (N_{cc}). Latitude (Lat) and longitude (Lon) are expressed in decimal degrees.
 554

Site code	Site Name	Region	Lat, Lon	<i>Heteractis magnifica</i>		<i>Stichodactyla mertensii</i>		<i>Entacmaea quadricolor</i>	
				N	N _{cc}	N	N _{cc}	N	N _{cc}
1	Gulf of Aqaba	North Red Sea	28.185, 34.638					5	5
2	Jazirat Burcan	North Red Sea	27.910, 35.065					24	24
3	An Numan	North Red Sea	27.139, 35.751	3	3			14	14
4	Nuwayshziyah	North Red Sea	26.624, 36.095					20	20
5	Mashabi	North Red Sea	25.582, 36.549	1	1			11	11
6	Abu Matari	North Red Sea	24.723, 37.151					1	1
7	Yanbu	North Red Sea	24.150, 37.675	3	1	13	13	5	5
8	Qita' Al-Girsh	Central Red Sea	22.436, 39.001	2		11	11	28	28
9	Shib Nazar	Central Red Sea	22.331, 38.863	2	1	7	7		
10	Fsar	Central Red Sea	22.227, 39.030	20	14			11	10
11	Abu Madafi	Central Red Sea	22.074, 38.778			6	6	1	1
12	Obhur	Central Red Sea	21.671, 38.844	8	5	25	25	3	3
13	South Reef (Al-Lith)	Central Red Sea	19.876, 40.114	7	3				
14	Lagoon2	South Red Sea	19.559, 40.055	1	1				
15	Abu Dauqa	South Red Sea	19.209, 40.109	1	1	5	5		
16	Dorish	South Red Sea	18.506, 40.670	3	3	4	4		
17	Sumayr	South Red Sea	17.787, 41.442	1	1	4	4		
18	Mamali Kabir	South Red Sea	17.605, 41.671			2	2		
19	Joey's Bluff	South Red Sea	17.476, 41.786	4	3	1	1		
20	Fi`ran	South Red Sea	17.177, 42.205			2	1		
21	Ghurab	South Red Sea	17.109, 42.069	2	1	2	2		
22	Baghlah	South Red Sea	16.980, 41.385	7	1	3	3		
23	Dhi Dahaya	South Red Sea	16.875, 41.440	7	4	5	5	7	7
24	Duraka	South Red Sea	16.860, 42.322	25	5				
25	Zahrat Durakah	South Red Sea	16.840, 42.305			1	1	3	3
26	Mazagnef	South Red Sea	16.592, 42.335	3	2				
27	Hindiya	South Red Sea	16.577, 42.240	4	3				
28	Dumsuq	South Red Sea	16.518, 42.041	11	5	1	1		
29	Djibouti	Gulf of Aden	12.221, 43.439	5	3	8	7		
30	Maldives	Indian Ocean	3.090, 72.976	6	6	3	3	4	4
31	Christmas Island	Indian Ocean	-10.460, 105.629			3	3		
32	Abrolhos Island	Indian Ocean	-28.790, 113.863					7	7
33	Tuare	Bismarck Sea	-5.087, 150.190	1	1	4	4	21	20
34	Kapeppa	Bismarck Sea	-5.091, 150.202					2	2
35	Kimbe Island	Bismarck Sea	-5.203, 150.374	51	51	5	5	5	5
36	Lizard Island	Coral Sea	-14.673, 145.451	1	1	7	7	3	3
37	Keppel Islands	Coral Sea	-23.155, 150.956					9	9
38	Northwest Island	Coral Sea	-23.280, 151.748					13	13
39	Heron Island	Coral Sea	-23.461, 151.934					6	6
40	North Solitary Island	Coral Sea	-29.925, 153.390					7	5
41	Lord Howe Island	Tasman Sea	-31.530, 159.077					39	28
42	Moorea	Pacific Ocean	-17.539, -149.830	26	13				
Total individuals				205	133	122	120	249	234

555 Table 2. Analysis of molecular variance results for *Heteractis magnifica*,
 556 *Stichodactyla mertensii*, and *Entacmaea quadricolor* sampled from across the Indo-
 557 Pacific. Sites with less than five specimens were not included in this analysis. Sites
 558 were also assigned to one of two regions prior to analysis, the Red Sea (here including
 559 Djibouti), and the rest of the Indo-Pacific.

Source of Variation	d.f.	SS	Variance	% of	F-statistic
<i>Heteractis magnifica</i>					
Among regions	2	75.8	0.519	14.3%	$F_{RT} = 0.143$ $F_{SR} = 0.113$
Among sites within regions	4	40.1	0.352	9.7%	$F_{ST} = 0.240$
Among individuals within sites	92	268.6	0.162	4.5%	$F_{IS} = 0.059$
Within individuals	99	257.0	2.596	71.6%	$F_{IT} = 0.285$
Total	197	641.6	3.629	100%	
<i>Stichodactyla mertensii</i>					
Among regions	1	72.4	1.651	41.8%	$F_{RT} = 0.408$ $F_{SR} = 0.019$
Among sites within regions	8	30.2	0.046	1.1%	$F_{ST} = 0.419$
Among individuals within sites	81	239.1	0.600	14.8%	$F_{IS} = 0.255$
Within individuals	91	159.5	1.753	43.3%	$F_{IT} = 0.567$
Total	181	501.3	4.050	100%	
<i>Entacmaea quadricolor</i>					
Among regions	2	249.7	1.029	22.1%	$F_{RT} = 0.220$ $F_{SR} = 0.064$
Among sites within regions	14	134.9	0.235	5.0%	$F_{ST} = 0.270$
Among individuals within sites	200	762.8	0.414	8.9%	$F_{IS} = 0.121$
Within individuals	217	648.0	2.986	64.0%	$F_{IT} = 0.359$
Total	433	1795.5	4.664	100%	

560

561

562 FIGURE LEGENDS

563 Figure 1. Numbered sampling sites (42) for *Heteractis magnifica*, *Stichodactyla*
564 *mertensii*, and *Entacmaea quadricolor* across the Indo-Pacific. Individual anemones
565 were sampled opportunistically, so not every species was sampled at each site. Size of
566 points is proportional to sample sizes. Specific information regarding the number of
567 specimens collected per site and other geographic information such as longitude and
568 latitude can be found in Table 1. Colours of points represent regions: Red Sea (blue),
569 Gulf of Aden (red), Indian Ocean (green), Bismarck Sea (purple), and Pacific Ocean
570 (orange). Photos of the three anemones are included, but it should be noted that
571 multiple morphotypes of *Entacmaea quadricolor* exist. Map created using an
572 equatorial projection centered on a prime Meridian with equally spaced straight
573 meridians and equal-area.

574

575 Figure 2. Structure output for *Heteractis magnifica*, *Stichodactyla mertensii*, and
576 *Entacmaea quadricolor* sampled from across the Indo-Pacific, for $K = 2$ to 4. Sites
577 are arranged from northwest to southeast. Numeric codes for each site correspond to
578 the codes used in Table 1. Major oceanographic regions are also indicated in a
579 coloured bar at the bottom of each graph for reference: Red Sea (blue), Gulf of Aden
580 (red), Indian Ocean (green), Bismarck Sea (purple), and Pacific Ocean (orange).

581

582 Figure 3. Results of Principal Components Analyses performed on the genetic data
583 from (a) *Heteractis magnifica*, (b) *Stichodactyla mertensii*, and (c) *Entacmaea*
584 *quadricolor* sampled from across the Indo-Pacific. Points are coloured according to
585 the oceanographic region of their origin. Major oceanographic regions are indicated in
586 the legend at the top: Red Sea (RS), Gulf of Aden (GA), Indian Ocean (IO), Bismarck
587 Sea (BS), and Pacific Ocean (PO). The values indicated along each axis correspond to
588 the percentage of inertia explained by the corresponding axis.

589

590 Figure 4. Scatterplots from the Isolation by Distance analysis comparing the pairwise
591 matrices of overwater geographic distance (in hundreds of km) and standardized
592 genetic distance (F'_{ST}) between sites with five or more *Heteractis magnifica* (yellow),
593 *Stichodactyla mertensii* (light blue), and *Entacmaea quadricolor* (grey) specimens,
594 within the Red Sea.

595

596

597

598 REFERENCES

- 599 Allen, G. R., Drew, J., & Fenner, D. (2010). *Amphiprion pacificus*, a new species of
600 anemonefish (Pomacentridae) from Fiji, Tonga, Samoa, and Wallis Island. *Aqua*,
601 *International Journal of Ichthyology*, *16*, 129–139.
- 602 Arbogast, B. S., & Kenagy, G. J. (2001). Comparative phylogeography as an integrative
603 approach to historical biogeography. *Journal of Biogeography*, *28*, 819–825.
604 <https://doi.org/10.1046/j.1365-2699.2001.00594.x>
- 605 Bay, L. K., Choat, J. H., van Herwerden, L., & Robertson, D. R. (2004). High genetic
606 diversities and complex genetic structure in an Indo-Pacific tropical reef fish
607 (*Chlorurus sordidus*): Evidence of an unstable evolutionary past? *Marine Biology*,
608 *144*, 757–767. <https://doi.org/10.1007/s00227-003-1224-3>
- 609 Benjamini, Y., & Hochberg, Y. (1995). Controlling the false discovery rate: A practical and
610 powerful approach to multiple testing. *Journal of the Royal Statistical Society, Series*
611 *B (Methodological)*, *57*, 289–300. [https://doi.org/10.1111/j.2517-](https://doi.org/10.1111/j.2517-6161.1995.tb02031.x)
612 [6161.1995.tb02031.x](https://doi.org/10.1111/j.2517-6161.1995.tb02031.x)
- 613 Bermingham, E., & Moritz, C. (1998). Comparative phylogeography: Concepts and
614 applications. *Molecular Ecology*, *7*, 367–369. [https://doi.org/10.1046/j.1365-](https://doi.org/10.1046/j.1365-294x.1998.00424.x)
615 [294x.1998.00424.x](https://doi.org/10.1046/j.1365-294x.1998.00424.x)
- 616 Billingham, M. R., Reusch, T. B. H., Alberto, F., & Serrão, E. A. (2003). Is asexual
617 reproduction more important at geographical limits? A genetic study of the seagrass
618 *Zostera marina* in the Ria Formosa, Portugal. *Marine Ecology Progress Series*, *265*,
619 77–83. <https://doi.org/10.3354/meps265077>
- 620 Bouwmeester, J., Gatins, R., Giles, E. C., Sinclair-Taylor, T. H., & Berumen, M. L. (2016).
621 Spawning of coral reef invertebrates and a second spawning season for scleractinian
622 corals in the central Red Sea. *Invertebrate Biology*, *135*, 273–284.
623 <https://doi.org/10.1111/ivb.12129>
- 624 Bowen, B. W., Gaither, M. R., DiBattista, J. D., Iacchei, M., Andrews, K. R., Grant, W. S., ...
625 Briggs, J. C. (2016). Comparative phylogeography of the ocean planet. *Proceedings*
626 *of the National Academy of Sciences*, *113*, 7962–7969.
627 <https://doi.org/10.1073/pnas.1602404113>
- 628 Bridge, T., Scott, A., & Steinberg, D. (2012). Abundance and diversity of anemonefishes and
629 their host sea anemones at two mesophotic sites on the Great Barrier Reef, Australia.
630 *Coral Reefs*, *31*, 1057–1062. <https://doi.org/10.1007/s00338-012-0916-x>
- 631 Brolund, T. M., Tychsen, A., Nielsen, L. E., & Arvedlund, M. (2004). An assemblage of the
632 host anemone *Heteractis magnifica* in the northern Red Sea, and distribution of the
633 resident anemonefish. *Journal of the Marine Biological Association of the United*
634 *Kingdom*, *84*, 671–674. <https://doi.org/10.1017/S0025315404009737h>
- 635 Chessel, D., Dufour, A. B., & Thioulouse, J. (2004). The ade4 package—I: One-table
636 methods. *R News*, *4*, 5–10.
- 637 Crandall, E. D., Frey, M. A., Grosberg, R. K., & Barber, P. H. (2008). Contrasting
638 demographic history and phylogeographical patterns in two Indo-Pacific gastropods.
639 *Molecular Ecology*, *17*, 611–626. <https://doi.org/10.1111/j.1365-294X.2007.03600.x>
- 640 Crandall, E. D., Riginos, C., Bird, C. E., Liggins, L., Treml, E., Beger, M., ... Gaither, M. R.
641 (2019). The molecular biogeography of the Indo-Pacific: Testing hypotheses with
642 multispecies genetic patterns. *Global Ecology and Biogeography*, *28*, 943–960.
643 <https://doi.org/10.1111/geb.12905>
- 644 Dawson, M. N., Louie, K. D., Barlow, M., Jacobs, D. K., & Swift, C. C. (2002). Comparative
645 phylogeography of sympatric sister species, *Clevelandia ios* and *Eucyclogobius*
646 *newberryi* (Teleostei, Gobiidae), across the California Transition Zone. *Molecular*
647 *Ecology*, *11*, 1065–1075. <https://doi.org/10.1046/j.1365-294X.2002.01503.x>

- 648 DiBattista, J. D., Choat, J. H., Gaither, M. R., Hobbs, J.-P. A., Lozano-Cortés, D. F., Myers,
649 R. F., ... Berumen, M. L. (2016). On the origin of endemic species in the Red Sea.
650 *Journal of Biogeography*, *43*, 13–30. <https://doi.org/10.1111/jbi.12631>
- 651 Dohna, T. A., Timm, J., Hamid, L., & Kochzius, M. (2015). Limited connectivity and a
652 phylogeographic break characterize populations of the pink anemonefish, *Amphiprion*
653 *perideraion*, in the Indo-Malay Archipelago: Inferences from a mitochondrial and
654 microsatellite loci. *Ecology and Evolution*, *5*, 1717–1733.
655 <https://doi.org/10.1002/ece3.1455>
- 656 Dunn, D. F. (1981). The clownfish sea anemones: Stichodactylidae (Coelenterata: Actiniaria)
657 and other sea anemones symbiotic with pomacentrid fishes. *Transactions of the*
658 *American Philosophical Society*, *71*, 3–115. <https://doi.org/10.2307/1006382>
- 659 Earl, D. A. (2012). STRUCTURE HARVESTER: A website and program for visualizing
660 STRUCTURE output and implementing the Evanno method. *Conservation Genetics*
661 *Resources*, *4*, 359–361. <https://doi.org/10.1007/s12686-011-9548-7>
- 662 Eckert, C. G. (2001). The loss of sex in clonal plants. *Evolutionary Ecology*, *15*, 501–520.
663 <https://doi.org/10.1023/A:1016005519651>
- 664 Fautin, D. G., & Allen, G. R. (1992). *Field guide to anemone fishes and their host sea*
665 *anemones*. Perth: Western Australian Museum.
- 666 Fautin, D. G., & Allen, G. R. (1997). *Anemone fishes and their host sea anemones: A guide*
667 *for aquarists and divers* (Rev. ed.). Perth: Western Australian Museum.
- 668 Frisch, A. J., Hobbs, J.-P. A., Hansen, S. T., Williamson, D. H., Bonin, M. C., Jones, G. P., &
669 Rizzari, J. R. (2019). Recovery potential of mutualistic anemone and anemonefish
670 populations. *Fisheries Research*, *218*, 1–9.
671 <https://doi.org/10.1016/j.fishres.2019.04.018>
- 672 Gaither, M. R., Bowen, B. W., Bordenave, T.-R., Rocha, L. A., Newman, S. J., Gomez, J. A.,
673 ... Craig, M. T. (2011). Phylogeography of the reef fish *Cephalopholis argus*
674 (Epinephelidae) indicates Pleistocene isolation across the Indo-Pacific barrier with
675 contemporary overlap in the coral triangle. *BMC Evolutionary Biology*, *11* (189).
676 <https://doi.org/10.1186/1471-2148-11-189>
- 677 Gaither, M. R., & Rocha, L. A. (2013). Origins of species richness in the Indo-Malay-
678 Philippine biodiversity hotspot: Evidence for the centre of overlap hypothesis.
679 *Journal of Biogeography*, *40*, 1638–1648. <https://doi.org/10.1111/jbi.12126>
- 680 Gatins, R., Saenz-Agudelo, P., Scott, A., & Berumen, M. L. (2018). Development and
681 characterization of new polymorphic microsatellite markers in four sea anemones:
682 *Entacmaea quadricolor*, *Heteractis magnifica*, *Stichodactyla gigantea*, and
683 *Stichodactyla mertensii*. *Marine Biodiversity*, *48*, 1283–1290.
684 <https://doi.org/10.1007/s12526-016-0576-0>
- 685 Giles, E. C., Saenz-Agudelo, P., Hussey, N. E., Ravasi, T., & Berumen, M. L. (2015).
686 Exploring seascape genetics and kinship in the reef sponge *Stylissa carteri* in the Red
687 Sea. *Ecology and Evolution*, *5*, 2487–2502. <https://doi.org/10.1002/ece3.1511>
- 688 Hall, R. (2002). Cenozoic geological and plate tectonic evolution of SE Asia and the SW
689 Pacific: Computer-based reconstructions, model and animations. *Journal of Asian*
690 *Earth Sciences*, *20*, 353–431. [https://doi.org/10.1016/S1367-9120\(01\)00069-4](https://doi.org/10.1016/S1367-9120(01)00069-4)
- 691 Hoffmann, R. J. (1986). Variation in contributions of asexual reproduction to the genetic
692 structure of populations of the sea anemone *Metridium senile*. *Evolution*, *40*, 357–
693 365. <https://doi.org/10.1111/j.1558-5646.1986.tb00477.x>
- 694 Holm, S. (1979). A simple sequentially rejective multiple test procedure. *Scandinavian*
695 *Journal of Statistics*, *6*, 65–70. Retrieved from JSTOR.
- 696 Hui, M., Kraemer, W. E., Seidel, C., Nuryanto, A., Joshi, A., & Kochzius, M. (2016).
697 Comparative genetic population structure of three endangered giant clams (Cardiidae:

- 698 *Tridacna* species) throughout the Indo-West Pacific: implications for divergence,
699 connectivity and conservation. *Journal of Molluscan Studies*, 82, 403–414.
700 <https://doi.org/10.1093/mollus/eyw001>
- 701 Huyghe, F., & Kochzius, M. (2017). Highly restricted gene flow between disjunct populations
702 of the skunk clownfish (*Amphiprion akallopisos*) in the Indian Ocean. *Marine*
703 *Ecology*, 38, e12357. <https://doi.org/10.1111/maec.12357>
- 704 Johannesson, K., & André, C. (2006). Life on the margin: Genetic isolation and diversity loss
705 in a peripheral marine ecosystem, the Baltic Sea. *Molecular Ecology*, 15, 2013–2029.
706 <https://doi.org/10.1111/j.1365-294X.2006.02919.x>
- 707 Jombart, T., Devillard, S., & Balloux, F. (2010). Discriminant analysis of principal
708 components: A new method for the analysis of genetically structured populations.
709 *BMC Genetics*, 11 (94). <https://doi.org/10.1186/1471-2156-11-94>
- 710 Kearse, M., Moir, R., Wilson, A., Stones-Havas, S., Cheung, M., Sturrock, S., ... Drummond,
711 A. (2012). Geneious Basic: An integrated and extendable desktop software platform
712 for the organization and analysis of sequence data. *Bioinformatics*, 28, 1647–1649.
713 <https://doi.org/10.1093/bioinformatics/bts199>
- 714 Kendall, M. G., & Smith, B. B. (1939). The problem of m rankings. *Annals of Mathematical*
715 *Statistics*, 10, 275–287. <https://doi.org/10.1214/aoms/1177732186>
- 716 Klausewitz, W. (1989). Evolutionary history and zoogeography of the Red Sea ichthyofauna.
717 In W. Büttiker & F. Krupp (Eds.), *Fauna of Saudi Arabia* (Vol. 10, pp. 310–337).
718 Basle, Switzerland: Pro Entomologia.
- 719 Kopelman, N. M., Mayzel, J., Jakobsson, M., Rosenberg, N. A., & Mayrose, I. (2015).
720 Clumpak: A program for identifying clustering modes and packaging population
721 structure inferences across K. *Molecular Ecology Resources*, 15, 1179–1191.
722 <https://doi.org/10.1111/1755-0998.12387>
- 723 Legendre, P., & Lapointe, F.-J. (2004). Assessing congruence among distance matrices:
724 Single-malt Scotch whiskeys revisited. *Australian & New Zealand Journal of*
725 *Statistics*, 46, 615–629. <https://doi.org/10.1111/j.1467-842X.2004.00357.x>
- 726 Leray, M., Beldade, R., Holbrook, S. J., Schmitt, R. J., Planes, S., & Bernardi, G. (2010).
727 Allopatric divergence and speciation in coral reef fish: The three-spot dascyllus,
728 *Dascyllus trimaculatus*, species complex. *Evolution*, 64, 1218–1230.
729 <https://doi.org/10.1111/j.1558-5646.2009.00917.x>
- 730 Litsios, G., Pearman, P. B., Lanterbecq, D., Tolou, N., & Salamin, N. (2014). The radiation of
731 the clownfishes has two geographical replicates. *Journal of Biogeography*, 41, 2140–
732 2149. <https://doi.org/10.1111/jbi.12370>
- 733 Ludt, W. B., & Rocha, L. A. (2015). Shifting seas: The impacts of Pleistocene sea-level
734 fluctuations on the evolution of tropical marine taxa. *Journal of Biogeography*, 42,
735 25–38. <https://doi.org/10.1111/jbi.12416>
- 736 Meirmans, P. G. (2006). Using the AMOVA framework to estimate a standardized genetic
737 differentiation measure. *Evolution*, 60, 2399–2402. <https://doi.org/10.1111/j.0014-3820.2006.tb01874.x>
- 739 Meirmans, P. G. (2015). Seven common mistakes in population genetics and how to avoid
740 them. *Molecular Ecology*, 24, 3223–3231. <https://doi.org/10.1111/mec.13243>
- 741 Nanninga, G. B., Saenz-Agudelo, P., Manica, A., & Berumen, M. L. (2014). Environmental
742 gradients predict the genetic population structure of a coral reef fish in the Red Sea.
743 *Molecular Ecology*, 23, 591–602. <https://doi.org/10.1111/mec.12623>
- 744 O'Donnell, J. L., Beldade, R., Mills, S. C., Williams, H. E., & Bernardi, G. (2017). Life
745 history, larval dispersal, and connectivity in coral reef fish among the Scattered
746 Islands of the Mozambique Channel. *Coral Reefs*, 36, 223–232.
747 <https://doi.org/10.1007/s00338-016-1495-z>

- 748 Otwoma, L. M., & Kochzius, M. (2016). Genetic population structure of the coral reef sea
749 star *Linckia laevigata* in the western Indian Ocean and Indo-West Pacific. *PLOS*
750 *ONE*, *11*, e0165552. <https://doi.org/10.1371/journal.pone.0165552>
- 751 Paradis, E., Claude, J., & Strimmer, K. (2004). APE: an R package for analyses of
752 phylogenetics and evolution. *Bioinformatics*, *20*, 289–290.
- 753 Peakall, P. E., & Smouse, R. (2012). GenAIEx 6.5: Genetic analysis in Excel. Population
754 genetic software for teaching and research—An update. *Bioinformatics*, *28*, 2537–
755 2539.
- 756 Pinsky, M. L., Montes, Jr., H. R., & Palumbi, S. R. (2010). Using isolation by distance and
757 effective density to estimate dispersal scales in anemonefish. *Evolution*, *64*, 2688–
758 2700. <https://doi.org/10.1111/j.1558-5646.2010.01003.x>
- 759 Pinsky, M. L., Saenz-Agudelo, P., Salles, O. C., Almany, G. R., Bode, M., Berumen, M. L.,
760 ... Planes, S. (2017). Marine dispersal scales are congruent over evolutionary and
761 ecological time. *Current Biology*, *27*, 149–154.
762 <https://doi.org/10.1016/j.cub.2016.10.053>
- 763 Pritchard, J. K., Stephens, M., & Donnelly, P. (2000). Inference of population structure using
764 multilocus genotype data. *Genetics*, *155*, 945–959.
- 765 Randall, J. E. (1998). Zoogeography of shore fishes of the Indo-Pacific region. *Zoological*
766 *Studies*, *37*, 227–268.
- 767 Raymond, M., & Rousset, F. (1995). GENEPOP (version 1.2): Population genetics software
768 for exact tests and ecumenicism. *Journal of Heredity*, *86*, 248–249.
- 769 Reimer, J. D., Herrera, M., Gatins, R., Roberts, M. B., Parkinson, J. E., & Berumen, M. L.
770 (2017). Latitudinal variation in the symbiotic dinoflagellate *Symbiodinium* of the
771 common reef zoantharian *Palythoa tuberculosa* on the Saudi Arabian coast of the
772 Red Sea. *Journal of Biogeography*, *44*, 661–673. <https://doi.org/10.1111/jbi.12795>
- 773 Richardson, D. L., Harriott, V. J., & Harrison, P. L. (1997). Distribution and abundance of
774 giant sea anemones (Actiniaria) in subtropical eastern Australian waters. *Marine and*
775 *Freshwater Research*, *48*, 59–66. <https://doi.org/10.1071/mf96020>
- 776 Rocha, L. A., Craig, M. T., & Bowen, B. W. (2007). Phylogeography and the conservation of
777 coral reef fishes. *Coral Reefs*, *26*, 501–512. [https://doi.org/10.1007/s00338-007-0261-](https://doi.org/10.1007/s00338-007-0261-7)
778 [7](https://doi.org/10.1007/s00338-007-0261-7)
- 779 Rousset, F. (2008). Genepop'007: A complete re-implementation of the Genepop software for
780 Windows and Linux. *Molecular Ecology Resources*, *8*, 103–106.
781 <https://doi.org/10.1111/j.1471-8286.2007.01931.x>
- 782 Saenz-Agudelo, P., DiBattista, J. D., Piatek, M. J., Gaither, M. R., Harrison, H. B., Nanninga,
783 G. B., & Berumen, M. L. (2015). Seascape genetics along environmental gradients in
784 the Arabian Peninsula: Insights from ddRAD sequencing of anemonefishes.
785 *Molecular Ecology*, *24*, 6241–6255. <https://doi.org/10.1111/mec.13471>
- 786 Sawall, Y., Al-Sofyani, A., Banguera-Hinestroza, E., & Voolstra, C. R. (2014). Spatio-
787 temporal analyses of *Symbiodinium* physiology of the coral *Pocillopora verrucosa*
788 along large-scale nutrient and temperature gradients in the Red Sea. *PLOS ONE*, *9*,
789 e103179. <https://doi.org/10.1371/journal.pone.0103179>
- 790 Scott, A. (2017). Sea Anemones. In R. Calado, I. Olivotto, O. M. Planas, & G. J. Holt (Eds.),
791 *Marine Ornamental Species Aquaculture* (pp. 437–456). Chichester, UK: John Wiley
792 & Sons, Ltd. <https://doi.org/10.1002/9781119169147.ch21b>
- 793 Scott, A., & Baird, A. H. (2015). Trying to find Nemo: Low abundance of sea anemones and
794 anemonefishes on central and southern mid-shelf reefs in the Great Barrier Reef.
795 *Marine Biodiversity*, *45*, 327–331. <https://doi.org/10.1007/s12526-014-0245-0>
- 796 Scott, A., & Harrison, P. L. (2005). Synchronous spawning of host sea anemones. *Coral*
797 *Reefs*, *24*, 208–208. <https://doi.org/10.1007/s00338-005-0488-0>

- 798 Scott, A., & Harrison, P. L. (2007). Embryonic and larval development of the host sea
799 anemones *Entacmaea quadricolor* and *Heteractis crispa*. *The Biological Bulletin*,
800 213, 110–121. <https://doi.org/10.2307/25066627>
- 801 Scott, A., & Harrison, P. L. (2009). Gametogenic and reproductive cycles of the sea anemone,
802 *Entacmaea quadricolor*. *Marine Biology*, 156, 1659–1671.
803 <https://doi.org/10.1007/s00227-009-1201-6>
- 804 Sebens, K. P. (1980). The regulation of asexual reproduction and indeterminate body size in
805 the sea anemone *Anthopleura elegantissima* (Brandt). *The Biological Bulletin*, 158,
806 370–382. <https://doi.org/10.2307/1540863>
- 807 Sheppard, C. R. C., Bowen, B. W., Chen, A. C., Craig, M. T., Eble, J., Fitzsimmons, N., ...
808 Yesson, C. (2013). British Indian Ocean Territory (the Chagos Archipelago): Setting,
809 Connections and the Marine Protected Area. In C. R. C. Sheppard (Ed.), *Coral Reefs*
810 *of the United Kingdom Overseas Territories* (pp. 223–240).
811 https://doi.org/10.1007/978-94-007-5965-7_17
- 812 Steinberg, R., van der Meer, M., Walker, E., Berumen, M. L., Hobbs, J.-P. A., & van
813 Herwerden, L. (2016). Genetic connectivity and self-replenishment of inshore and
814 offshore populations of the endemic anemonefish, *Amphiprion latezonatus*. *Coral*
815 *Reefs*, 35, 959–970. <https://doi.org/10.1007/s00338-016-1420-5>
- 816 Timm, J., & Kochzius, M. (2008). Geological history and oceanography of the Indo-Malay
817 Archipelago shape the genetic population structure in the false clown anemonefish
818 (*Amphiprion ocellaris*). *Molecular Ecology*, 17, 3999–4014.
819 <https://doi.org/10.1111/j.1365-294X.2008.03881.x>
- 820 Titus, B. M., Benedict, C., Laroche, R., Gusmão, L. C., Van Deusen, V., Chiodo, T., ...
821 Rodríguez, E. (2019). Phylogenetic relationships among the clownfish-hostingsea
822 anemones. *Molecular Phylogenetics and Evolution*, 139, 106526.
823 <https://doi.org/10.1016/j.ympev.2019.106526>.
- 824 van der Meer, M. H., Jones, G. P., Hobbs, J.-P. A., & van Herwerden, L. (2012). Historic
825 hybridization and introgression between two iconic Australian anemonefish and
826 contemporary patterns of population connectivity. *Ecology and Evolution*, 2, 1592–
827 1604. <https://doi.org/10.1002/ece3.251>
- 828 Vogler, C., Benzie, J., Barber, P. H., Erdmann, M. V., Ambariyanto, Sheppard, C. R. C., ...
829 Wörheide, G. (2012). Phylogeography of the crown-of-thorns starfish in the Indian
830 Ocean. *PLOS ONE*, 7, e43499. <https://doi.org/10.1371/journal.pone.0043499>
- 831 Voris, H. K. (2000). Maps of Pleistocene sea levels in Southeast Asia: Shorelines, river
832 systems and time durations. *Journal of Biogeography*, 27, 1153–1167.
833 <https://doi.org/10.1046/j.1365-2699.2000.00489.x>
- 834 Weir, B. S., & Cockerham, C. C. (1984). Estimating F-statistics for the analysis of population
835 structure. *Evolution*, 38, 1358–1370. <https://doi.org/10.1111/j.1558-5646.1984.tb05657.x>
- 837 Wright, S. (1965). The interpretation of population structure by F-statistics with special
838 regard to systems of mating. *Evolution*, 19, 395–420. <https://doi.org/10.1111/j.1558-5646.1965.tb01731.x>

840 BIOSKETCH

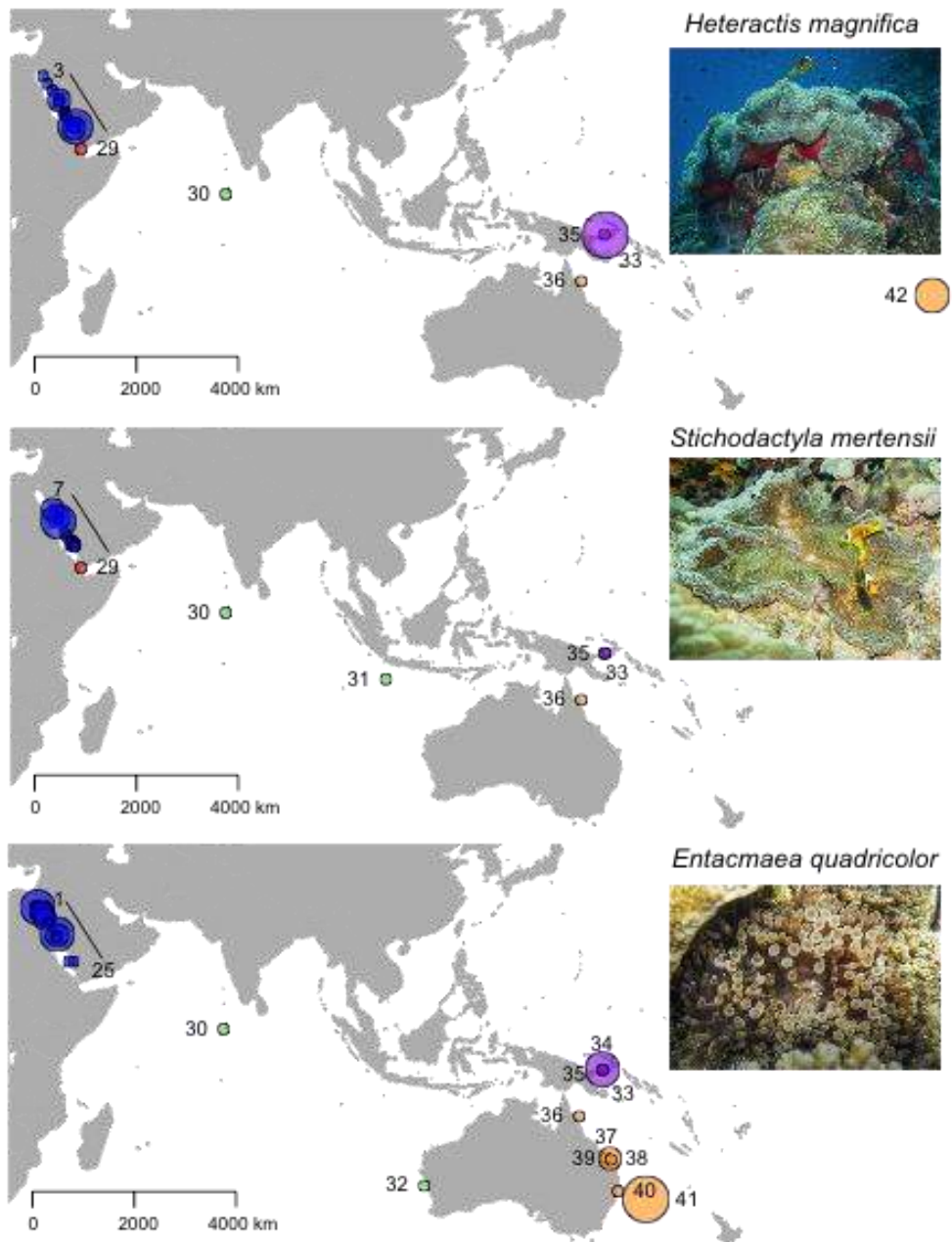
841 Madeleine A. Emms is interested in studying population structure,
842 connectivity, and demography in coral reef systems. All other co-authors are broadly
843 interested in the ecology, evolution and conservation of coral reefs. PSA and MLB
844 conceived and designed the study. RAG and PSA carried out the laboratory work.
845 MAE, ECG, and PSA analysed the data. MAE and PSA led the writing of the

846 manuscript with assistance from ECG and MLB. All authors contributed tissue
847 specimens and contributed to the manuscript.

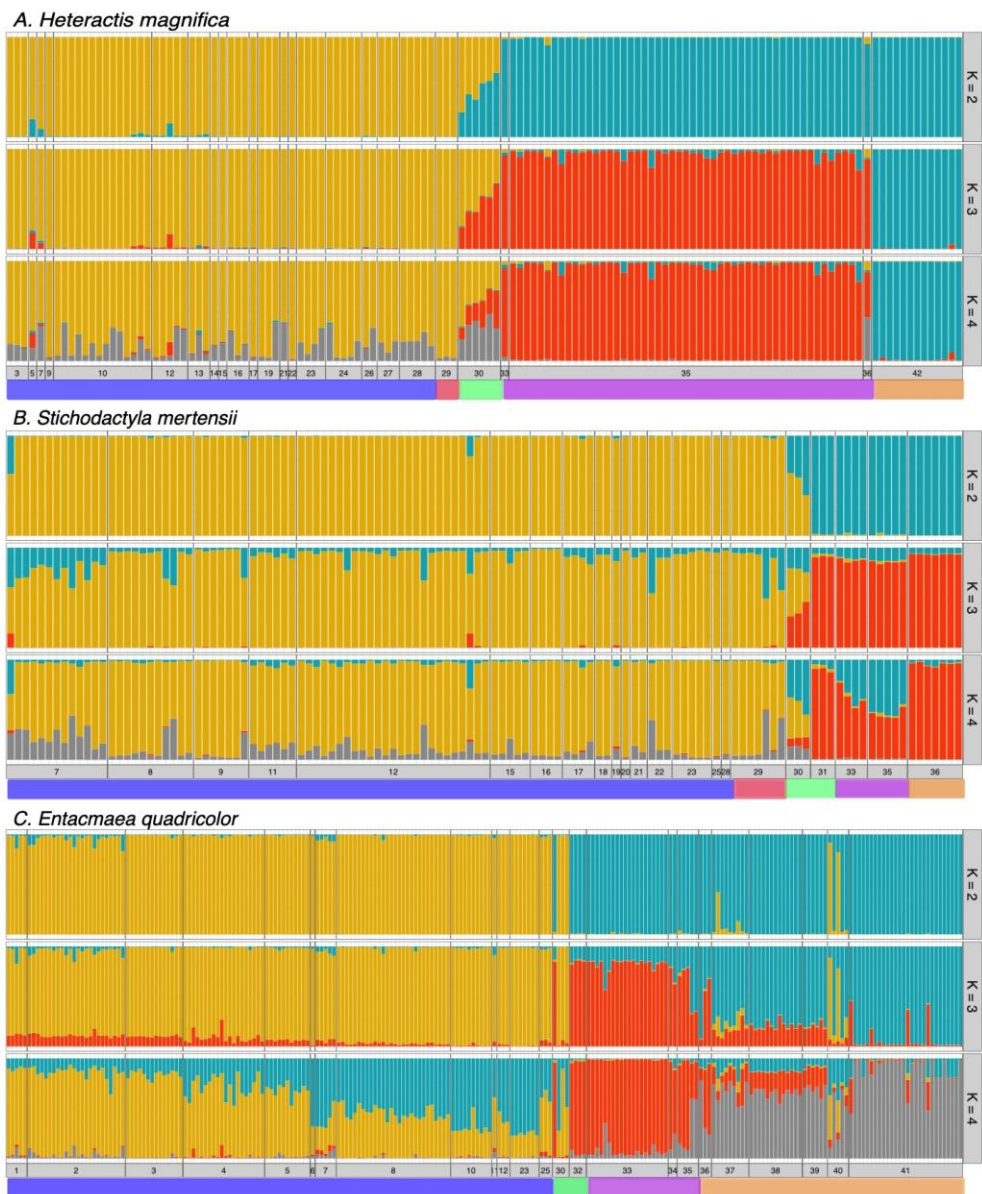
848

849

850 Figure 1



851
852
853
854
855
856
857
858
859
860
861
862
863
864



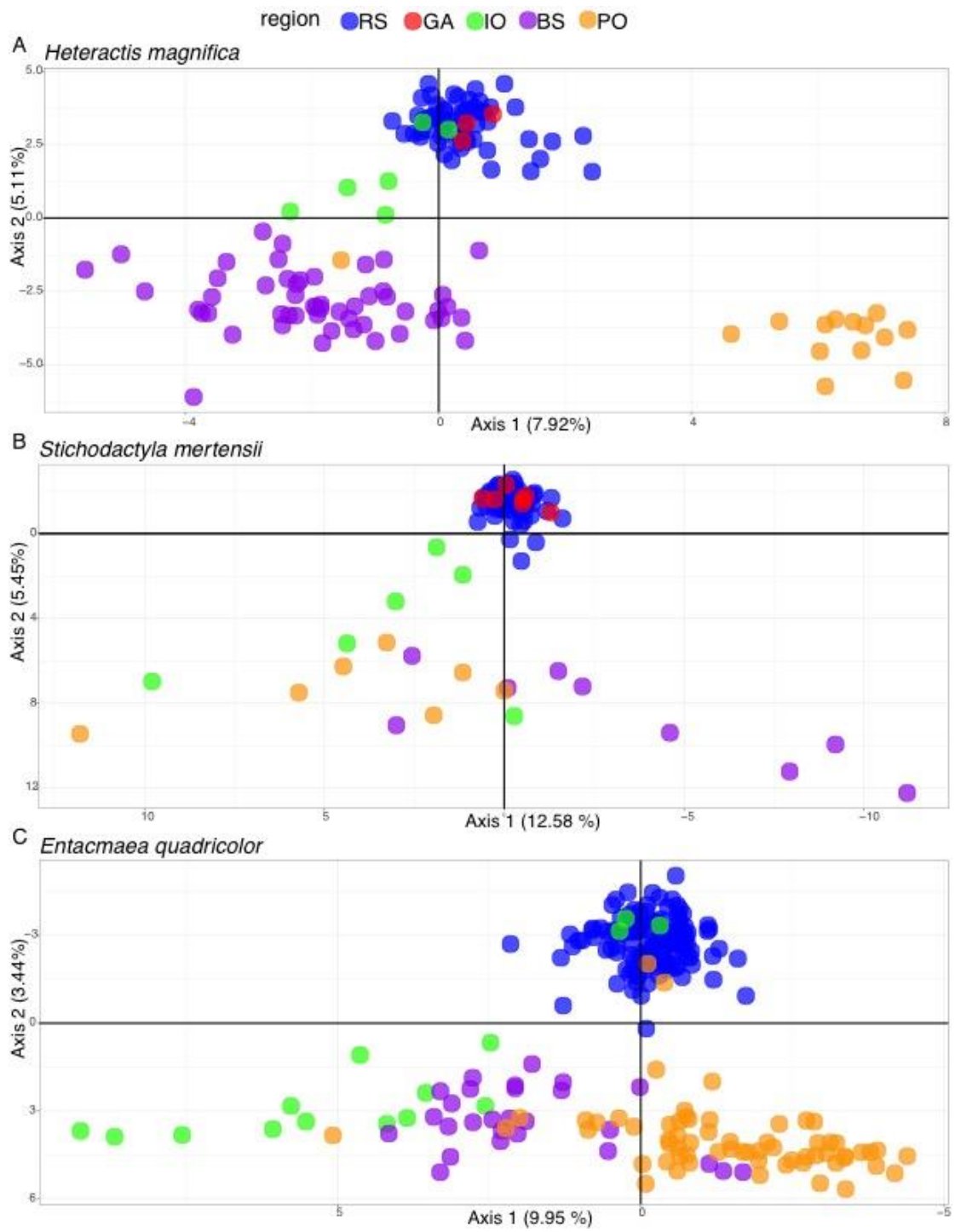
866

867

868

869

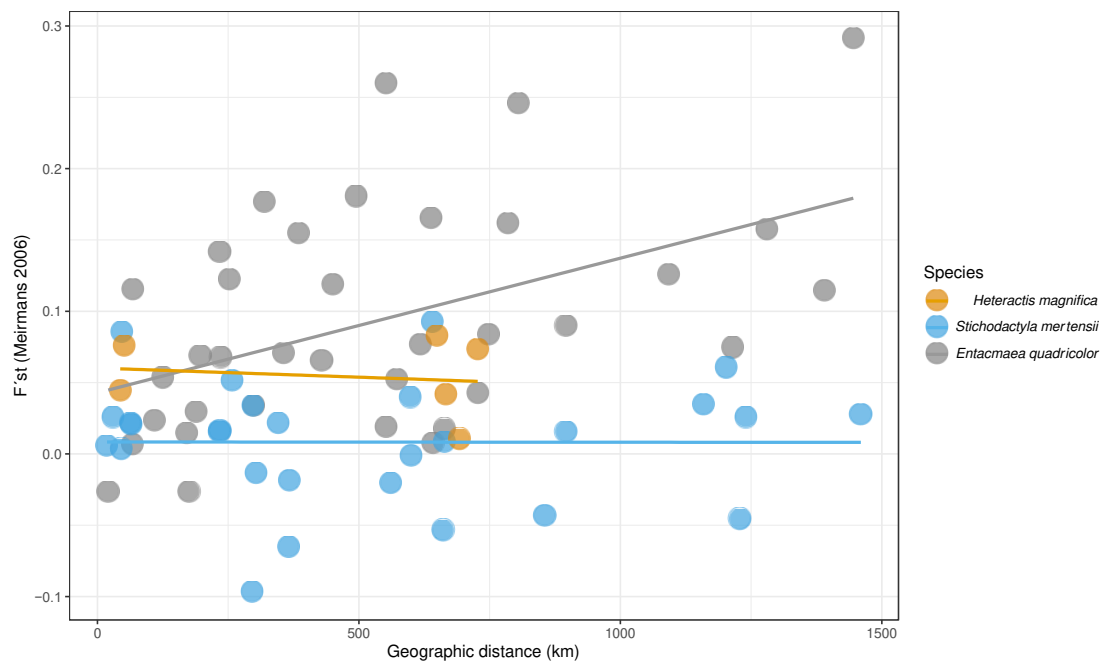
870 Figure 3



871

872

873 Figure 4



874